scientific reports

Check for updates

OPEN

Exploring the organic nature, morphological plasticity and ecological significance of Aster like nanoparticles

Maxime Fuster[1], Hermine Billard[1], Jérémie Mathurin[2], Ariane Deniset-Besseau[2], David Albertini[3], Télesphore Sime-Ngando[1] & Jonathan Colombet[1]✉

The smallest entities in aquatic ecosystems, i.e., femtoplankton, are certainly the largest reservoir of uncharacterized biodiversity. Among them, the discovery of mysterious Aster like nanoparticles has raised many questions about their nature, origin and ecology. Here, we highlight the original nature of this new model, organic and composed of enriched-calcium carbohydrates, with no detection of nucleic acids or proteins. The biosynthesis of these entities seems to be associated with a host in their 11 arms' form prior to their release into the environment. An intriguing aspect of their mode of development is their ability, once free, to change form and maintain their abundance autonomously without metabolism being detected, resulting in an unexpected polymorphism. Their remarkable capacity for massive in situ development and their links with prokaryotes and other microbes suggest a major role in the functioning of aquatic ecosystems. There's no doubt that these new entities are a source of new knowledge not only in the sciences of organic nanoparticles, but also in their ecological importance for aquatic ecosystems.

Aster like nanoparticles (ALNs) are mysterious entities discovered in 2019 in aquatic environments[1]. Data collected to date have shown the existence of distinct ALN morphotypes depending on the number and form of arms present. The dominant forms have 4, 11 or 20 arms, with 11-armed representatives possibly featuring a bud[1]. A remarkable intrinsic feature is that their size (on average from 110 to 430 nm) and volume (less than 1.4×10^{-3} µm^3) are below the minimum required for life expression (TMCV, i.e., 8×10^{-3} µm^3), yet they are able to maintain themselves in numbers in the absence of microorganisms, prokaryotes or eukaryotes[1]. Their ecology is characterized by, (i) their ability to colonize different continental and coastal aquatic environments with a high level of eutrophication[2], (ii) massive bloom production, with peak abundances of up to $9.0 \pm 0.5 \times 10^7$ ALNs.mL^{-1}, and (iii) covariation with prokaryotes[1,3]. These original characteristics make ALNs uncharacterized planktonic entities and potential major players in the functioning of aquatic ecosystems. However, these preliminary data are fragmentary and the intrinsic nature and ecological features of ALNs remain to be determined. In this work, we studied the biochemical characteristics and genesis (under controlled conditions) of these entities, coupled with a detailed analysis of their morphological diversity. A multi-year ecosystem approach on several lakes enabled us to approach their ecology and their role in matter fluxes. The results showed (i) a greater diversity of forms than initially mentioned[1], (ii) an original biochemical composition with the absence of detection of hereditary genetic support and metabolism, (iii) an interconversion of forms articulated around a complex mode of development and (iv) major functional importance in aquatic ecosystems, notably in the bioavailable calcium cycle.

ALNs are original organic nanoparticles

The morphological diversity of ALNs previously reported mentioned the existence of three dominant shapes[1]. Although a minority in number under in situ conditions, here we revealed a wider range of shapes and sizes including: a cross shape form two times smaller in length (50 nm) than the smallest recorded, intermediate shapes whose number of arms varies from 6 to 11 including shapes with an overextended non-budding arm, and intriguing ALNs with two or three bud-like appendices (Supplementary Figure S1). The different shapes of ALNs appear to be distributed along a gradient of complexity from the cross shape to the 20-armed shape.

[1]Laboratoire Microorganismes: Génome et Environnement (LMGE), UMR CNRS 6023, Université Clermont-Auvergne, 63000 Clermont-Ferrand, France. [2]Institut de Chimie Physique, CNRS UMR 8000, Université Paris-Saclay, 91405 Orsay, France. [3]CNRS, INSA Lyon, Ecole Centrale de Lyon, CPE Lyon, INL, UMR5270, Université Claude Bernard Lyon 1, 69622 Villeurbanne, France. ✉email: jonathan.colombet@uca.fr

TEM X-ray diffraction analysis showed an elemental composition C15/O5/Ca different from prokaryotes (C408/O48/Ca) or virus like particles (VLPs) (C89/O21/Ca) (Fig. 1A), with a pronounced calcium (Ca) enrichment notably 26 times greater than prokaryotes. It is important to underline the very low level of P (< 0.02%) and absence of detection of N, markers of proteins and nucleic acids. The recorded C/N/P ratio were of 6137/0/1, 59/9/1 and 33/6/1 for ALN, prokaryotes and VLPs respectively, consistent with an enrichment in protein (enriched in nitrogen) and nucleic acids (enriched in both nitrogen and phosphorus) for prokaryotes and VLPs[4] compared to ALNs. Atomic force microscopy (AFM) imaging coupled with infra red (IR) analysis showed a flexible amorphous appearance and an organic nature, suspected in our pionneer work[1] (Fig. 1B, C). 59 spectra were obtained on a isolated ALN in the different part of the entity (Fig. 1C). The spectra showed a clear homogeneity of the ALN composition as the spectra have been taken all along the entity and all of them present the same absorption bands. The analysis of these spectra showed clear features similar with various polysaccharrides absorption associated with Ca^{2+} ions[5,6]. First there was clear carbohydrate absorption signal as the various C-O-C absorption bands were represented (bands around 1040 cm^{-1} and 1110 cm^{-1}). In addition to these bands, two major absorption bands could be observed: one around 1410 cm^{-1} the other around 1625 cm^{-1} which are compatible with a IR absorption of carboxylic acid associated with Ca^{2+} ions. The attribution of the polysaccharide nature cannot be assessed perfectly due to the limited spectral range of the AFM-IR measurement made here. However a good hypothetic candidate can be carrageenans as the absorption band around 1205 cm^{-1} and 1260 cm^{-1} can be associated with a S=O absorption caracteristic to this molecule family[7,8] and these molecules are known to be associated with Ca^{2+} ions[9]. Even if there was an ester band absorption, the presence of esterfied lipids cannot be assessed due to the lack of clear C-H absorptions. The absence of amide I and II absorption as well as the absence of a strong absorption band around 1240 cm^{-1} can exclude the presence of both proteins and nucleic acids in ALN.

The bromination capacity of ALNs confirmed their organic nature[10] (Supplementary Figure S2) and their ability to complex ions. Ca atoms undoubtedly play a major role in the molecular arrangement of carbohydrates and in the three-dimensional structure of ALNs. This role remains to be specified. The lack of AFM-IR detection of nucleic acids and proteins rules out the presence of an intrinsic hereditary genetic support and the presence of metabolism, leaving open the question of their origin.

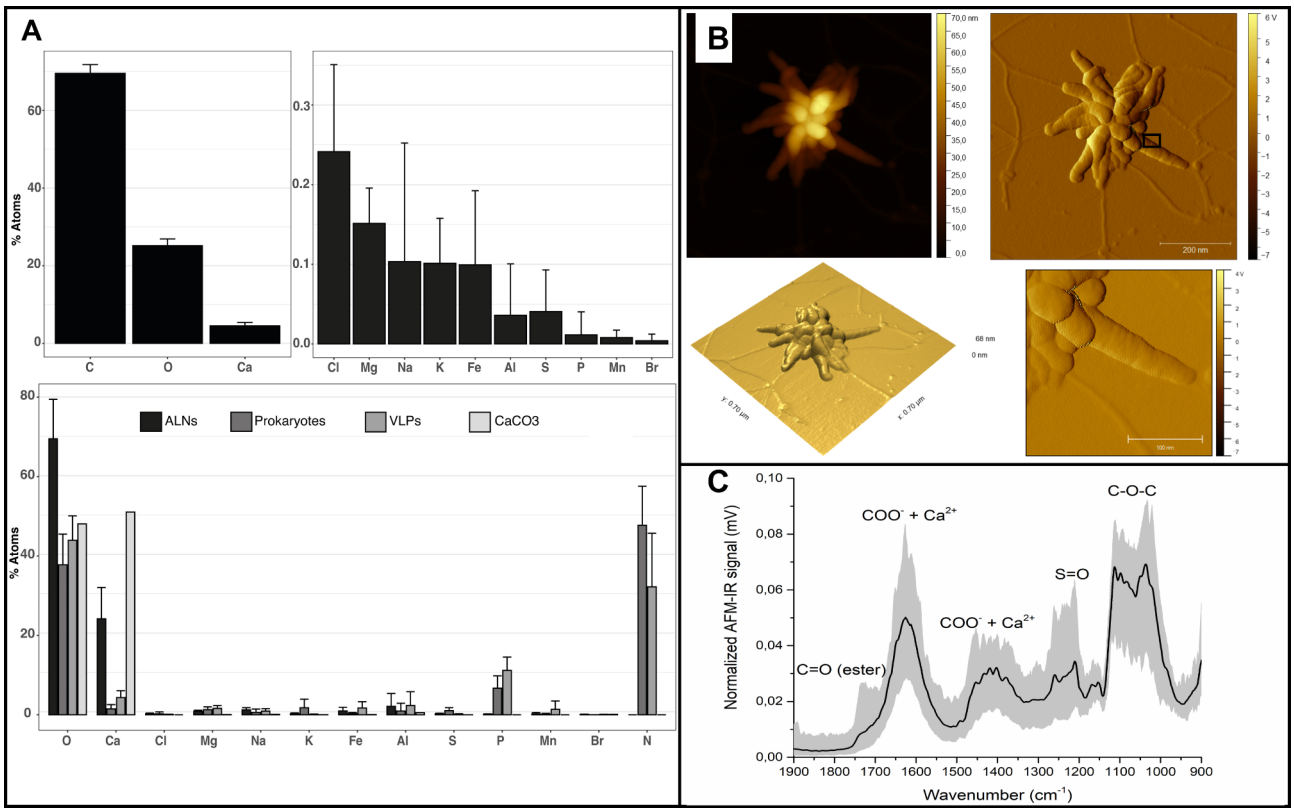

Fig. 1. X-ray analysis by transmission electron microscopy (X-ray TEM) and atomic force microscopy (AFM) revealed organic nature of ALNs with an original biogeochemical composition. (**A**) X-ray TEM analysis showed the original elemental composition (± standard deviation) of ALNs (black bars on the 3 histograms), compared with prokaryotes (Prok), virus-like particles (VLPs) and CaCo3. (**B**) AFM topographic and 3D images of ALNs revealed amorphous appearance. (**C**) AFM-IR spectra obtained on an isolated ALN with a lateral resolution of around 25 nm: 59 spectra were averaged, the black line represents the average spectrum, the grey area represents the dispersion of the spectra obtained.

A complex development mode

In order to explore how ALNs develop, from genesis to degeneration, we investigated the potential links between their different ALN morphotypes, by monitoring long-term (120 days) variations in their abundances under different conditions (Fig. 2, Supplementary Table S1). While ALN concentrations remained stable between the start and the end of the incubations (Kruskal-Wallis test, $p > 0.01$), we observed significant variations in the proportions of the different morphotypes in all incubations (Fig. 2). These observations suggest that ALNs have a high degree of morphological plasticity, with potential shape changes during development.

In the absence of potential microbial hosts (i.e., under axenic condition), with ALNs enriched in cross and 5–10 armed shapes, we did not record the appearance of large shapes (11-budding armed and 20-armed ALNs) at day 120, while the ALN concentration remained stable (Fig. 2, Supplementary Table S1). These results suggest that the smallest ALNs maintain themselves autonomously, but without any increase in size associated with organic synthesis. Regeneration from a severed ALN (supported by existence of 6- to 11-armed shapes with an overextended non-budding arm), seems the most likely hypothesis.

In non-axenic, microorganism-rich conditions, which we separated into 4 conditions (C8, C10, C20, SN20) according to the sedimentation properties of the microorganisms and ALNs, from the largest (micro-eukaryotes, large prokaryotes, large ALNs concentrated in condition C8) to the smallest (small prokaryotes, small ALNs concentrated in condition SN20)[11], we reported the appearance and multiplication of the largest ALN shapes (20-armed) on day 120 (Fig. 2). These were greatest in conditions C8 and C10 with the highest densities of microorganisms at t0 (Fig. 2). The formation of the largest forms of ALN seems to require the presence of microorganisms. These observations suggest that large ALNs could be produced by microorganisms rather than small ALNs.

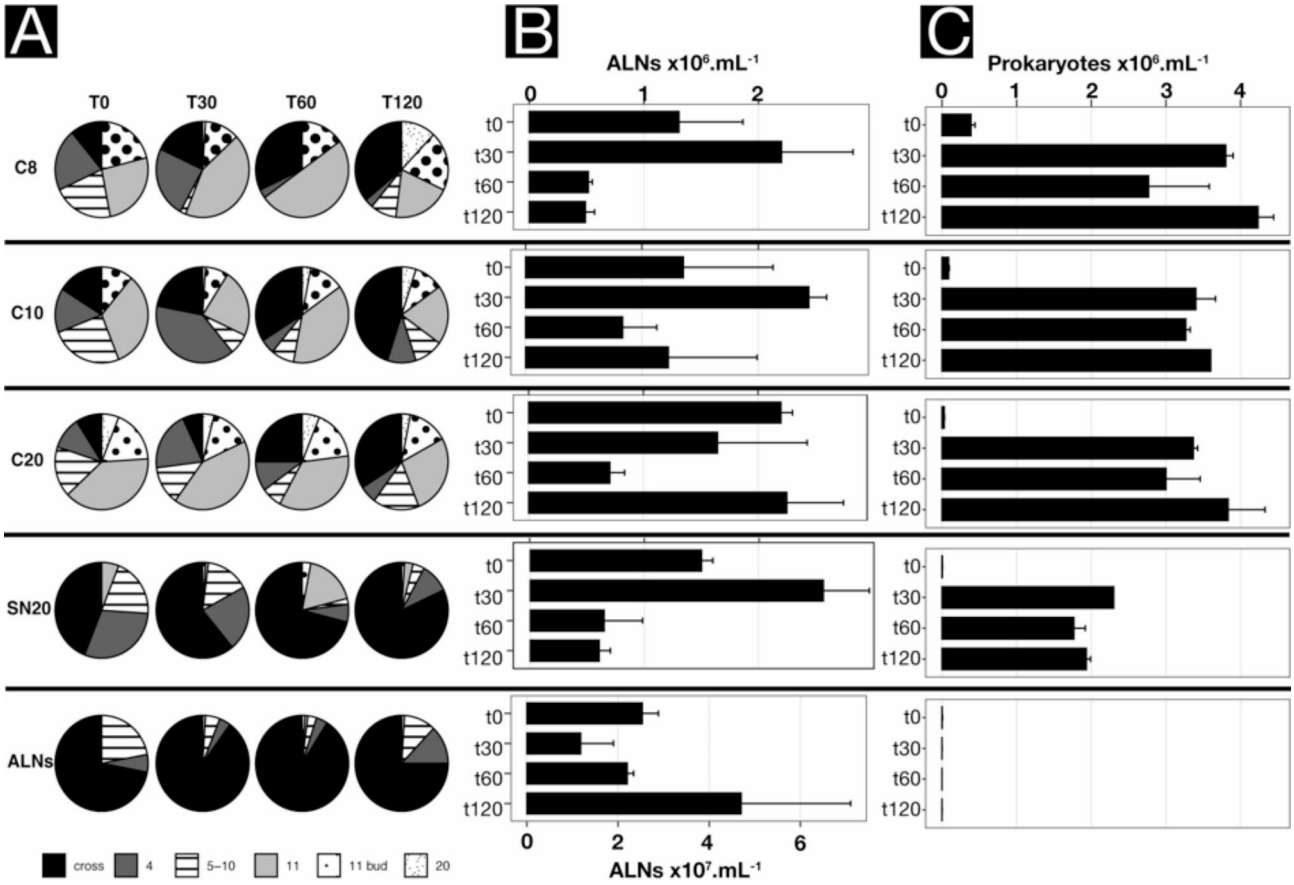

Fig. 2. : Evolution over 120 days (t0, t30, t60, t120) of the proportion of different ALN morphotypes (**A**), their abundances (**B**) and the abundance of prokaryotes (**C**) under 5 different incubation conditions (non-axenic, i.e., microorganims enriched, conditions : C8, C10, C20 and SN20, and axenic condition : ALNs). 11 :11-armed ALN, 11bud :11-budding armed ALN, 5–10 :5–10 -armed ALN, 20 :20-armed ALN, 4 :4-armed ALN articulated around an excrescence, cross : cross-shaped ALN. C8, C10, C20, corresponded respectively to the successive centrifugation pellets of a non-axenic ALN culture (8,000; 10,000 then 20,000 x g). SN20 corresponded to the supernatant of 20,000 x g obtained in the last step of centrifugation. ALNs corresponding to ALNs under axenic conditions, i.e., SN20 filtered at 0.2 µm and concentrated on unit 100 kDa molecular weight cut off (MWCO).

Under non-axenic conditions, many forms of ALNs were recorded with a bud-like outgrowth (11-budding armed). These could contribute to the observed maintenance of ALN concentrations through an alternative autonomous developmental capacities driven by budding.

Finally, the increase in the proportions of the smallest cross shape of ALNs (Khi2 test, $p < 0.01$), under all conditions, probably reflects the degradation of the largest forms in cross shape.

These data suggest that the different forms of ALNs are articulated according to a complex developmental pattern involving interconversion of forms and production in association with a microorganism. This is consistent with the supposed absence of metabolism and intrinsic genetic support for organic synthesis.

In this regard, we have reported original observations of ALNs (in the form 11-budding armed) appearing to emerge in an orderly fashion from spherical structures obtained after concentration by tangential ultrafiltration (Supplementary Figure S3). These structures have not been observed in the untreated lake sample and could therefore be the result of the destruction of hosts by the ultrafiltration step. Indeed, the mechanical effects of tangential ultrafiltration, which drives a pressurized medium at high speed parallel to a porous membrane to concentrate entities by separating them from the aqueous matrix, can result in the destruction of non-shock-resistant entities. This hypothesis was confirmed by the frequent observations, in lake samples, of numerous 11-armed ALNs associated with large cells (< 20 µm), without any specific identification of them (Supplementary Figure S4). These observations suggest that the primary production of ALNs takes place in the form of 11 budding armed within a cell.

Finally, we also reported the original observation of prokaryotes interacting with ALNs, and in particular ALN debris or cross ALN inside prokaryotes (Supplementary Figure S5). These images suggest that ALNs may be degraded by prokaryotes after phagocytosis. Processes of prey phagocytosis have recently been documented in a planktomycetes bacterium[12]. These ALN-prokaryote interactions remain putative and will need to be explored to be validated, which will require the as yet unattained ability to grow ALNs or purify them without any chemical or biological contaminants.

Taken together, these elements suggest a two-phases mode of ALN development, as proposed in Fig. 3 : a host-assisted production phase and an autonomous, regressive phase, with form interconversions and multiplication by budding. Budding could be the consequence of the detachment of budding arms, which can lead to the production of a new ALN (4 armed then 5–10 or 11 armed) of smaller size than the initial ALN. Prokaryotes could play a role in ALN recycling by digest.

This supposed mechanism of genesis and development remains to be proven but it raises fundamental questions about the autonomous phase. How do ALNs bud and change morphotype? To our knowledge, no non-metabolizing aquatic organic particle presents such a capacity. Extracellular molecular self-assembly of polysaccharides could be a plausible explanation for ALN shape change. Such molecules have been shown to be capable of self-assembly[13]. Finally, while a host-assisted reproductive phase is probable, we do not know the

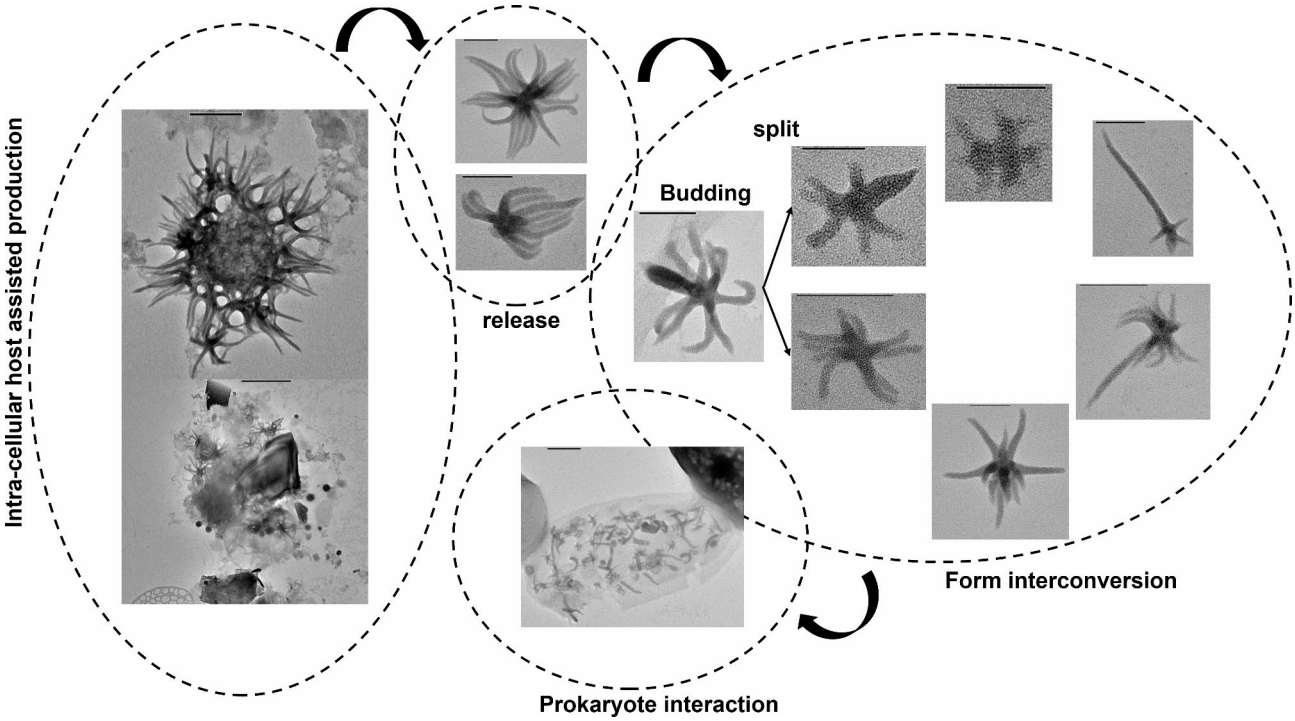

Fig. 3. : Proposal for a development mode of ALNs. A phase of intracellular production assisted by the host seems to be at the origin of the ALNs, which after bursting from the host are released into the environment. The free ALNs enter an autonomous and regressive phase, with interconversions of forms and multiplication by budding. Prokaryotes may play a role in ALN recycling.

underlying mechanisms. Do ALNs enter the host as a parasite or a symbiont? Or are they intrinsically produced under the sole control of the host? Finally, the alternative that it is a set of self-assembled subcellular components that can be easily reassimilated, disassembled and digested by living cells will also have to be considered.

A prominent ecological significance

The ecological impact of ALNs stems from their multi-year dynamics, with the appearance of massive blooms (up to $1.4 \pm 0.1 \times 10^8$ ALNs mL^{-1}) that were not reproducible from one year to the next (Fig. 4A). The control of these blooms was biological in nature, with strong correlations recorded with prokaryotes and micro-eukaryotes, particularly autotrophic types (Fig. 4B). These data reinforce the hypothesis of a tripartite relationship between ALNs/micro-eukaryotes/prokaryotes described above, although the identity of the interactants remains unknown. Rapid growth and decay (with temporal symmetry) of these blooms contrasts with the relative stability recorded over the long term under controlled conditions, indicating rapid production (up to 13 million ALNs produced per day per mL)/consumption or decay (up to 14 million ALNs consumed or recycled per day per mL). These values are similar to those recorded for production and decay of similar-sized entities (viruses) in freshwater[14,15], and suggest a key role for ALNs in the fitness of their producers and recyclers. Given their very high Ca load, these original transfers undoubtedly play a key role in the bioavailable Ca cycle of aquatic environments. We estimate that up to a 1.4 µg of organic Ca per liter could be released into the water per day in the form of ALN. At the peak of recorded ALN abundance (1.4×10^8 ALNs mL^{-1} in Fargette Lake), the organic Ca content sequestered by ALNs could represent 15 µg of Ca per liter, twice as much as that contained in prokaryotes.

Conclusions

Our work highlights the originality of ALNs, both intrinsically and ecologically. ALNs present an original biochemistry composed of calcium-enriched carbohydrates, with no detectable trace of protein or nucleic acids. Despite their supposed lack of metabolism, they are able to change morphotype and maintain themselves autonomously. Their relationship with prokaryotes and other microbial hosts, and their ability to transfer metallic elements such as Ca, coupled with a seasonality marked by high punctual abundances, make them a new player in the functioning of food webs that will need to be integrated into the modeling of matter and energy

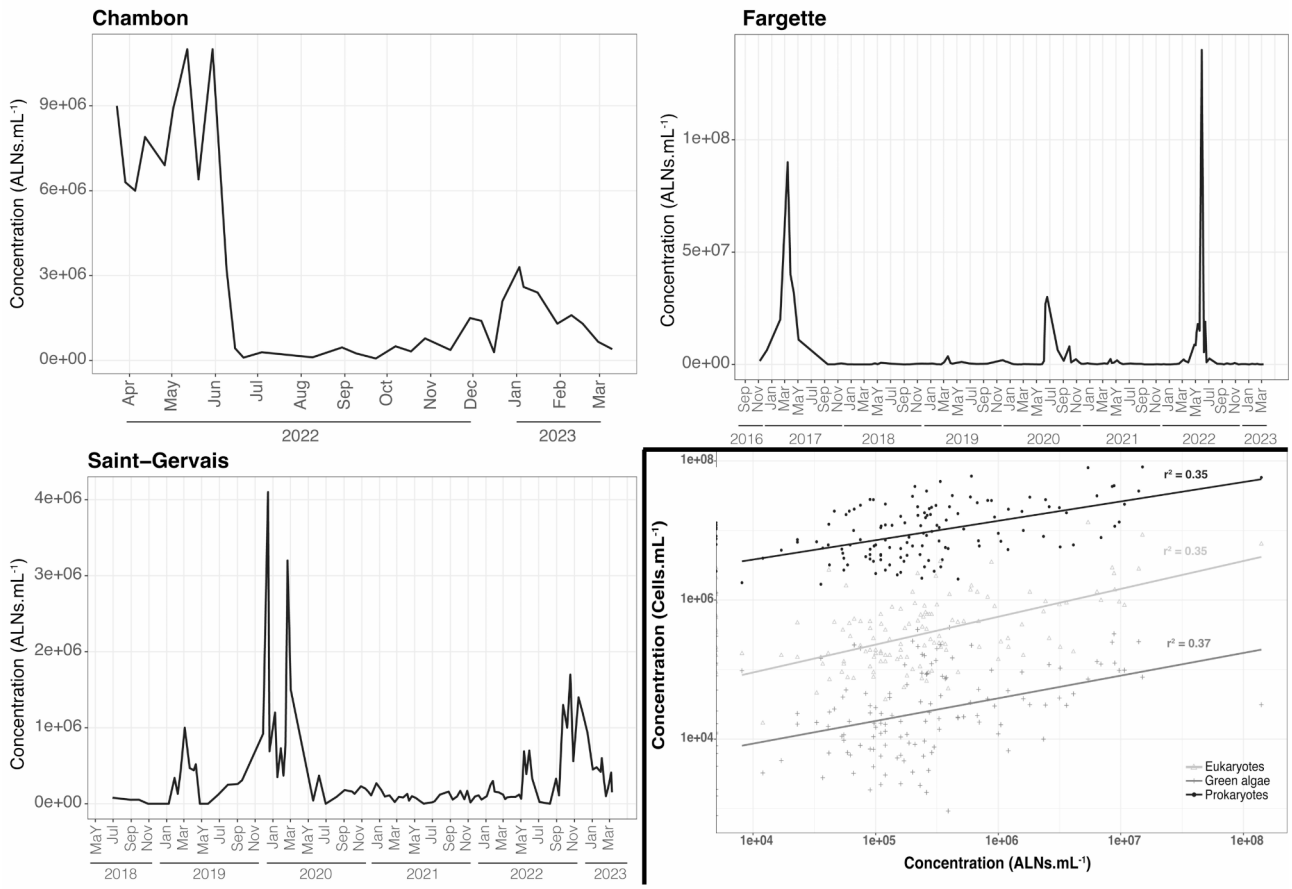

Fig. 4. : Temporal variations of ALN abundance in lake Chambon (34 time points), lake Fargette (128 time points) and lake Saint-Gervais (107 time points) (**A**) and Spearman correlation analyses with environmental parameters measured (**B**).

flows through aquatic systems. These original characteristics make ALNs new organic models which, as far as we know, do not correspond to any other organic entity described to date (prokaryotes, viruses, prions, nanobes), nor to any nanoparticle or organic component listed. These new models could be a source of new knowledge and applications, but further work is needed to determine their exact nature, for the taxonomic identification of their producer or interactant, and thus clarify their development mode and exact role in the environment.

Methods

Study sites

Samples were collected at the surface (0–40 cm) of three artificial freshwater lakes: Fargette (45°44'39"N; 3°27'21"E; 465 m altitude; surface area 1.2 ha; maximum depth 2.5 m), Chambon (45°50'22"N; 3°30'17"E; 490 m altitude; surface area 12 ha; maximum depth 6 m) and Saint-Gervais-d'Auvergne (SG) (46°02'15"N; 2°48'43"E; 680 m altitude; surface area 10.5 ha; maximum depth 4.5 m) during a temporal survey described below. These lakes are in the French Massif Central (within a 120 km radius). Fargette is a hyper eutrophic lake while SG and Chambon are eutrophic recreational lakes.

Morphological characterization and quantification of Aster like nanoparticles (ALNs)

ALNs in 1% (v/v) formaldehyde fixed samples were collected by centrifugation at 20,000 x *g* for 20 min at 14 °C directly onto 400-mesh electron microscopy copper grids covered with carbon-coated Formvar film (AO3X, Pelanne Instruments, Toulouse, France). Particles were over-contrasted using uranyl salts as described elsewhere[16]. Detection, characterization and quantification of ALNs, and their different forms, were realized in triplicates by transmission electron microscopy (TEM) using a Jeol JEM 2100-Plus microscope (JEOL, Akishima, Tokyo, Japan) operating at 80 kV and x50,000 to x150,000 magnifications as described in Colombet et al.[1]. The average biovolume of ALNs was calculated from the measurement of 212 ALNs contained in the ALN culture as described in Colombet et al.[1].

Biochemical characterization

Atomic force microscopy

Atomic Force Microscopy (AFM) were performed with a Bruker Dimension 3100 and Nanoscope V electronics in air. The imaging mode was intermittent contact mode with MikroMasch OPUS 240 tips (Nanoandmore France). Samples were deposited on freshly cleaved mica using a micrometric pipette (20µL). Observations were made 1 h after deposition to facilitate solvent evaporation.

Infrared-atomic force microscopy

AFM-IR analyses have been performed using a new system called IconIR (Bruker nano, Santa Barbara CA, USA) which allows high AFM performance (30 pm rms topography) with low thermal drift allowing to do scan size down to 100 nm. In this setup, the IR beam was focused on the topside of the sample onto the AFM cantilever. The system was coupled to a multi-chip quantum cascade laser source (MIRcat, Daylight Solutions; tunable repetition rates range of 0–2 MHz; spectral resolution of 0.1 cm^{-1}) that covers a portion of the mid-IR range, from 1900 cm^{-1} to 900 cm^{-1}. The data were acquired using the tapping AFM-IR mode described in Mathurin et al.[17]. The cantilever used here are the Tap300GB-G, 300 kHz, 40 N/m, Budget Sensors. The acquisition was made with the following protocol: after a AFM acquisition, the tip position was fixed on various positions of the ALN sample and the laser was tune on the whole spectral range. By looking the signal obtained for each wavenumber it was possible to reconstruct local absorption spectrum with a resolution around 25 nm. For each point 4 spectra have been obtained and averaged.

Bromination

Within two hours of the start of bromination, ALNs contained in the supernatant of the culture mentionned below centrifugated at 8,000 x g for 20 min at 14 °C were collected by centrifugation at 10,000 x g for 20 min at 14 °C. The pellet was 10-fold diluted in culture medium (see below) and incubated during 48 h after added of potassium bromide 3 M final concentration (BioUltra, Sigma Aldrich, MERCK, Darmstadt, Germany). An untreated sample served as control. Elemental analysis was realized at the end of the incubation as decribed below.

Elemental analysis

Elemental analysis was performed by energy dispersive X-ray (EDX) using the X-Max 80 mm^2 Large Area SDD Silicon Drift Detector (Oxford Instruments, Abingdon-on-Thames, United Kingdom) at 200 kV on a Jeol JEM 2100-Plus TEM (JEOL, Akishima, Tokyo, Japan). The elemental composition of 63 ALNs compared to 68 prokaryotes, 40 viral like particles and CaCO3 was deduced from the analysis of unfixed and unstained deposits from Lake or culture samples (collected by centrifugation as described above) on 3×3 10 nm thick window silicon nitride grids (SN100-A10Q33 Delta Microscopies, Mauressac, France) for C analysis or on 400-mesh copper grids coated with carbon-coated Formvar film (AO3X, Pelanne Instruments, Toulouse, France) for other elements. The elemental analysis for bromination were obtained on 5 ALNs (in each treatment) on 400 mesh copper grids covered with a carbon-coated Formvar film after deposit as described above.

The mass of Ca per ALN was obtained by multiplying the average measured volume of ALNs (122 580 nm^3) by the mass of a Ca atom divided by the atomic volume of the chemical constituents of the ALNs (deduced from the EDX analysis, related to one Ca atom: C15O5Ca).We apply a correction factor of 8/9 inherent to the lumen volumes obtained after observations of ultrathin sections in TEM. The average mass of Ca per ALN was estimated at 0.11 fg.

The mass of Ca per prokaryote was obtained by dividing the mass of C per prokaryote (i.e., 20 fg C, (17)) by the product of the mass of one C atom by the mass of one Ca atom by 408 (deduced from EDX analysis of prokaryotes showing a C/Ca ratio of 408).

Experimental monitoring

Enrichment and culture of ALNs

Sample collected on February 18th 2019 from Lake Saint-Gervais was used for enrichment and culture of ALNs. Within two hours after sampling, 60 L of water was filtered through a 25-µm-pore-size nylon mesh and filtrate was immediately concentrated by tangential-flow ultrafiltration using a Kross-Flow system (Spectrum, Breda, The Netherlands) equipped with a 0.2-µm cut-off cartridge. Aliquots of this concentrated 0.2–25 µm fraction were sequentially centrifuged[11] at 8,000 x g, 10,000 x g (pellets discarded), 12,000 x g then 15,000 x g for 20 min each time at 14 °C. ALNs contained in the pellets of these two last runs were pooled, amended with culture medium, filtered onto PES stericup 0.22 µm (Merck Millipore, Darmstadt, Germany), and cultivated at 4 °C in the dark for 32 months with a regular supply of culture medium. To obtain this culture medium, ultrafiltrate < 0.2 µm of the initial lake sample was filtered through a 30 kDa cut-off cartridge and autoclaved.

Growth monitoring

In the two hours before the start of monitoring, ALNs and associated microbial communities contained in the culture mentionned above were enriched and fragmented by sequential centrifugations[11] at 8,000 x g, 10,000 x g then 20,000 x g for 20 min each time at 14 °C. The centrifugation pellets (named respectively C8, C10, and C20), an aliquot of the 20,000 x g supernatant (named SN20), and an aliquot of the SN20 filtered onto 0.22 µm to remove prokaryotes and concentrated on Amicon Ultra-15 (Merck Millipore, Darmstadt, Germany) centrifugal filter units of 100 kDa MWCO (named ALNs) were finally diluted in 15 mL of culture medium. Thus, 5 fractions were obtained, 4 non-axenic (C8, C10, C20 and SN20 with selection on the size of potential host communities and ALNs) and one axenic (ALNs). These were inoculated in triplicates for 120 days in the dark at 4 °C. Samples at 0, 30, 60 and 120 days are taken and 1% final concentration formaldehyde-fixed before quantification of each ALN morphotype and of prokaryotes.

Ecological dynamic

Sample collections

Samples were collected at the surface (0–40 cm) during temporal survey of 7 years for Fargette (11-2016 to 02-2023), 5 years for SG (06-2018 to 02-2023), 1 year for Chambon (03-2022 to 02-2023). St. Gervais has the particularity of having been emptied during November, December 2018 and January 2019 and returned to its maximum depth in December 2019. During the empty period, samples were taken from a permanent puddle at the center of the lake supplied by the upstream source flowing into the lake. Samples of virus-like particles (VLPs), prokaryotes and ALNs were immediately fixed with 1% (v/v) formaldehyde and stored at 4 °C until counts. Unfixed samples for analyses of phytoplanktonic communities were transported at 4 °C and treated in the 4 h following sampling.

Abiotic parameters measurements

Dissolved oxygen content ($mg.L^{-1}$) and temperature (°Celsius) were measured in-situ with a submersible probe (ProDSS YSI, Yellow Springs, Ohio, USA), while pH was measured in the laboratory (probe Thermo Scientific, Orion Star A111, Waltham, MA).

Biotic parameters measurements

Phytoplanktonic communities. Pigment content was calculated ($\mu g\ L^{-1}$) using a submersible spectrofluorometric probe (BBE FluoroProbe, Moldaenke GmbH, DE). Counts of picophytoplankton populations (Green algae, Cyanobacteria, Cryptophyta were determined by flow cytometry according to the modified method of Marie et al.[18]. using a BD LSR Fortessa X-20 (BD Sciences, San Jose, CA). Photosynthetic cells were categorized into three sub-populations (Green algae, Cyanobacteria, Cryptophyta) according to their pigment content. Fluorescence signals from chlorophyll (Chl), phycoerythrin (PE) and phycocyanin (PC) were collected using 405 nm (50mW), 561 nm (50mW) and 640 nm (40 mW) lasers and 670/30, 586/15 and 670/14 filters respectively. Green algae correspond to cells containing only chlorophyll, Cyanobacteria is the sum of PE-rich and PC-rich cyanobacteria, Cryptophyta corresponds to populations whose major pigment is PE.

Prokaryote, eukaryotes and VLP counts. Counts of prokaryotes, eukaryotes and VLPs from fixed samples were performed in triplicates by flow cytometry according to Brussaard[19] using a BD FACSAria Fusion SORP (BD Sciences, San Jose, CA USA) equipped with an air-cooled laser, delivering 50 mW at 488 nm with 502 longpass, and 530/30 bandpass filter set-up.

All data were acquired and analyzed with BD FACSDiva 9.0 software.

Data analysis

All the statistical analyses were performed using R software (v.4.1.3). Differences in the ALN composition were determined by Wilcoxon test. The differential abundances of the forms of ALNs, between the different sampling times for each fraction, were determined using a χ^2 test. The effect of time on ALNs concentration was tested using a Kruskal-Wallis analysis. Their representation was performed using "ggplot2" packages. The potential links between ALNs and the accompanying environmental parameters were tested with Spearman correlations.

Data availability

All data generated or analyzed during this study are included in this published article or supplementary file. All other data that support the findings of this study are available from the corresponding author on reasonable request.

Received: 20 February 2024; Accepted: 16 September 2024
Published online: 27 September 2024

References

1. Colombet, J. *et al.* Discovery of high abundances of aster-like nanoparticles in pelagic environments: Characterization and dynamics. *Front. Microbiol.* **10**, 2376 (2019).
2. Fuster, M. *et al.* Trophic conditions influence widespread distribution of aster-like nanoparticles within aquatic environments. *Microb. Ecol.* **80**, 741–745 (2020).
3. Fuster, M., Billard, H., Bronner, G., Sime-Ngando, T. & Colombet, J. Occurrence and seasonal dynamics of ALNs in freshwater lakes are influenced by their biological environment. *Microb. Ecol.* https://doi.org/10.1007/s00248-022-01974-1 (2022).
4. Jover, L. F., Effler, T. C., Buchan, A., Wilhelm, S. W. & Weitz, J. S. The elemental composition of virus particles: Implications for marine biogeochemical cycles. *Nat. Rev. Microbiol.* **12**, 519–528 (2014).
5. Guo, X., Duan, H., Wang, C. & Huang, X. Characteristics of two calcium pectinates prepared from citrus pectin using either calcium chloride or calcium hydroxide. *J. Agric. Food Chem.* **62**, 6354–6361 (2014).
6. Yamakita, E. & Nakashima, S. Water retention of calcium-containing pectin studied by quartz crystal microbalance and infrared spectroscopy with a humidity control system. *J. Agric. Food Chem.* **66**, 9344–9352 (2018).
7. Wen, C. *et al.* Calcium-induced-gel properties for ι-carrageenan in the presence of different charged amino acids. *LWT* **146**, 111418 (2021).
8. Dordevic, D. *et al.* Edible/biodegradable packaging with the addition of spent coffee grounds oil. *Foods* **12**, 2626 (2023).
9. Michel, A.-S., Mestdagh, M. M. & Axelos, M. A. V. Physico-chemical properties of carrageenan gels in presence of various cations. *Int. J. Biol. Macromol.* **21**, 195–200 (1997).
10. Cantillo, D. & Kappe, C. O. Halogenation of organic compounds using continuous flow and microreactor technology. *React. Chem. Eng.* **2**, 7–19 (2017).
11. Colombet, J., Billard, H., Fuster, M. & Sime-Ngando, T. A practical guide to separate and concentrate ALNs and femtoplankton entities. *J. Microbiol. Methods* **211**, 106769 (2023).
12. Shiratori, T., Suzuki, S., Kakizawa, Y. & Ishida, K. Phagocytosis-like cell engulfment by a planctomycete bacterium. *Nat. Commun.* **10**, 5529 (2019).
13. Myrick, J. M., Vendra, V. K. & Krishnan, S. Self-assembled polysaccharide nanostructures for controlled-release applications. *Nanotechnol. Rev.* **3** (2014).
14. Fischer, U. & Velimirov, B. High control of bacterial production by viruses in a eutrophic oxbow lake. *Aquat. Microb. Ecol.* **27**, 1–12 (2002).
15. Mei, M. L. & Danovaro, R. Virus production and life strategies in aquatic sediments. *Limnol. Oceanogr.* **49**, 459–470 (2004).
16. Borrel, G. *et al.* Unexpected and novel putative viruses in the sediments of a deep-dark permanently anoxic freshwater habitat. *ISME J.* **6**, 2119–2127 (2012).
17. Mathurin, J. *et al.* How to unravel the chemical structure and component localization of individual drug-loaded polymeric nanoparticles by using tapping AFM-IR. *Analyst* **143**, 5940–5949 (2018).
18. Marie, D., Rigaut-Jalabert, F. & Vaulot, D. An improved protocol for flow cytometry analysis of phytoplankton cultures and natural samples. *Cytom. Pt A* **85**, 962–968 (2014).
19. Brussaard, C. P. D. Optimization of procedures for counting viruses by flow cytometry. *Appl. Environ. Microbiol.* **70**, 1506–1513 (2004).

Acknowledgements

This project has received financial support from the CNRS through the MITI interdisciplinaryprograms. We also benefited from (i) the CPER 2015–2020 SYMBIOSE challenge program(French Ministry of Research, UCA, CNRS, INRA, Auvergne-Rhone-Alpes Region, FEDER)which supported M.F. PhD fellowship and (ii) funding from the French government IDEX-ISITEinitiative 16-IDEX- 0001 (CAP 20–25). We would like to thank the CYSTEM-UCA Partnerplatform (Clermont Ferrand) and the Consortium Lyon Saint-Etienne de Microscopie (CLYM, FED 4092) for the access to the AFM.

Author contributions

J.C. conducted the study, which was initiated alongside by M.F., H.B. and T.S-N. J.C., M.F. and H.B. carried out the ALN culture, experimental monitoring and seasonal dynamics. J.C. carried out transmission electron microscopy imaging, EDX elemental analysis and bromination. J.C. and M.F. carried out transmission electron microscopy counting. J.C. and H.B. carried out flow cytometric analyis. J.M. and A.D-B. carried out atomic force microscopy-infrared analysis. D.A. performed atomic force microscopy imaging. All authors contributed to interpreting the data and writing the manuscript.

Declarations

Competing interests

The authors declare no competing interests.

Additional information

Supplementary Information The online version contains supplementary material available at https://doi.org/10.1038/s41598-024-73332-9.

Correspondence and requests for materials should be addressed to J.C.